Failure mechanism of anchored retaining wall due to the anchor head itself being broken





Kazuya Itoh, Naotaka Kikkawa & Yasuo Toyosawa
Construction Safety Research Group, National Institute of Occupational Safety and Health, Japan (JNIOSH), Tokyo, Japan

Naoaki Suemasa & Toshiyuki Katada
Department of Civil Engineering, Tokyo City University, Tokyo, Japan

ABSTRACT: In this research, a case history of temporary earth support collapse is first illustrated briefly and the mechanisms of accident occurrences are introduced, with the results showing that the shallow penetration of piles mainly caused the sequences of collapse. In order to understand these failure characteristics and mechanisms, centrifuge model tests using an in-flight excavator were carried out. The failure mechanism of the retaining wall in this labour accident was firstly demonstrated using centrifuge model tests by Toyosawa et al. (1998). In this paper, we added some viewpoints regarding the mechanism of the retaining wall and it was thus clarified that the active and passive earth pressures in the retaining wall increased during excavation and then the anchor head exceeded the capacity with respect to tensile stress. As a result, the retaining wall and ground behind the wall collapsed suddenly.

1 INTRODUCTON

Accidents due to collapse frequently occur during ground excavation. The need to decrease these accidents is currently a major concern not only in Japan, but also in several other countries as well.

Firstly, a case history has been described in which a temporary earth support collapsed and the ground behind the support failed. A total soil volume of 200 m^3 with a maximum thickness of 4 m slid into an excavation area and as a result five workers were killed and two others were injured.

Secondly, in the laboratory, the model ground in front of the anchored retaining wall was excavated using an in-flight excavator in a centrifugal field. Based on the results of two centrifuge model tests, the deformation characteristics, the earth pressure and failure mechanisms are discussed in this paper.

2 CASE HISTORY OF THE TEMPORARY EARTH SUPPORT COLLAPSE

2.1 *Outline of the construction work*

This accident occurred at the building construction site which had an excavation area width of 17.6 m and length of 30.3 m as shown in Figure 1. Figure 2 shows the results of a boring log geological survey.

The main piles were used as a temporary earth support system with the lateral wooden sheeting method. The length and the interval of the main piles were 15 m and 1 m, respectively. The diameter of the ground anchors was 117 mm, the length

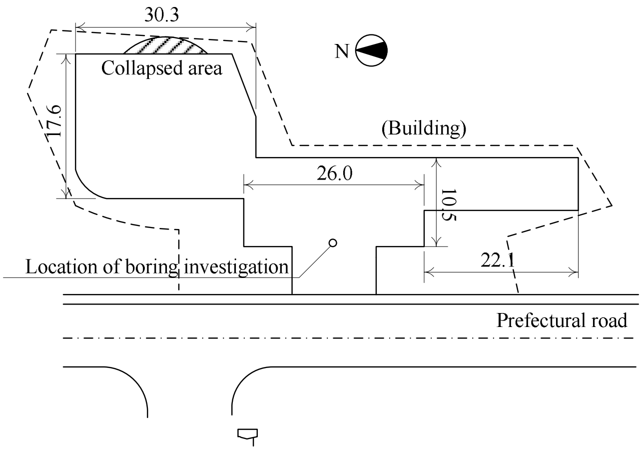

Fig. 1 The ground plan and location for the boring investigation

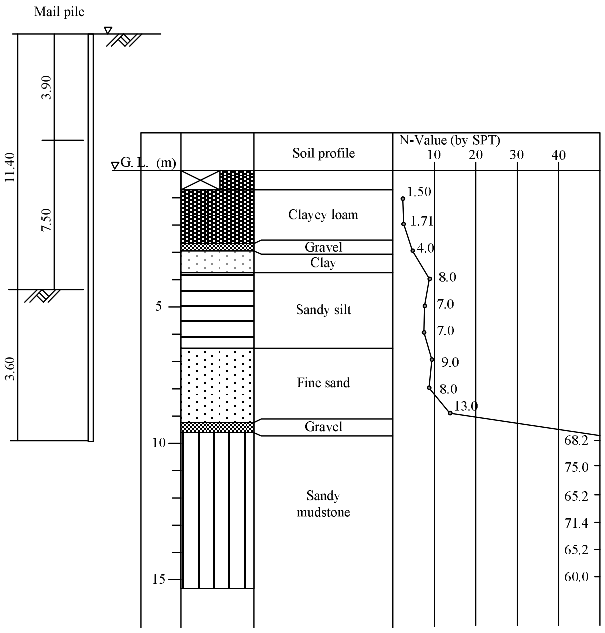

Fig. 2 Boring log of the construction site

was 20.5 m (effective length 5.0 m), the angle was 45 degrees and the horizontal interval of the anchors was 2.5 m.

2.2 *Situation relating to the accident occurrence*

In the morning that the accident occurred, at around 10:00 a. m., workers noticed that some H-steel piles on the east side had not penetrated below the excavation bottom. The engineer in charge felt there was a danger of a collapse, and he tried to reinforce the main piles with additional remedial piles and blind concrete.

At around 1:15 p.m., with a loud noise, the central 15 m of the temporary earth support structure on the east side collapsed suddenly with the ground behind the support. The ground slid into the excavation area with a soil volume of approximately 200 m^3 and a maximum thickness of approximately 4 m.

(a) The scene of the collapse accident (from south side)

(b) The scene of the collapse accident (from north side)

(c) Damaged H- steel for anchor head

Fig. 3 The scene of the collapse accident

Due to this collapse, eleven H- steel piles toppled. Four workers at the bottom of the excavation site were buried alive and three workers were struck by H- steel piles. As a result, five workers were killed and two others were injured.

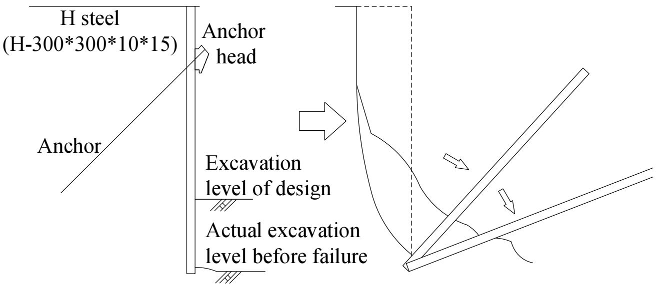

Fig. 4 Estimated mechanism of the collapse

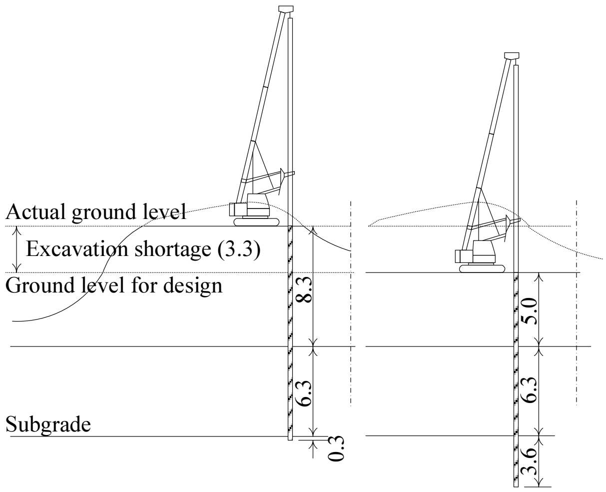

Fig. 5 The cause of a shortage of embedded depth of sheet pile walls

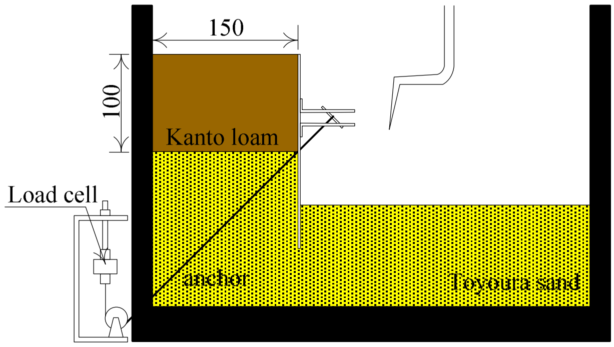

Fig. 6 Cross section of profile of two layers

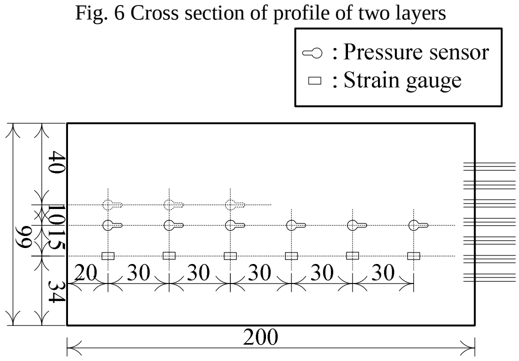

Fig. 7 Model of sheet pile wall

2.3 *Estimation of the mechanism of the collapse*

The sequence of collapse is shown schematically in Fig. 4. The mechanism of collapse is summarized as follows;

1) Remedial work was being performed on the excavation bottom despite insufficient penetration of the main piles. It is assumed that, due to insufficient penetration, the earth pressure caused the displacement of the main piles.
2) The main piles were supported by the ground anchors installed at an angle of 45 degrees from the horizontal plane. Downward force provided from the anchor's tensile force made the connection between the wale which supported the anchor heads and the anchor heads ineffective.
3) Finally, the unstable earth support structure led to a huge-volume soil collapse.

The cause of insufficient penetration of the main piles was shortage of excavation at the upper site; due to an engineering error which disregarded the plane of design as shown in Figure 5.

2.4 *Monitoring*

Instrumentation is usually required to monitor the performance of a sheet pile structure during construction. Measurements of movements and pressures furnish valuable information for use in verifying design assumptions. Most importantly, the data may forewarn of a potentially dangerous situation that could affect the stability of the structure. In this construction site, however, only visual inspection was used, such as checking for unusual surface signs.

3 CENTRIFUGE MODEL TESTS

3.1 *JNIOSH NIIS Mark II Centrifuge*

Centrifuge model tests were conducted to examine the failure mechanism of this accident, such as the retaining wall supported to ground anchors. All the tests described here were conducted using the JNIOSH NIIS Mark II Centrifuge (Horii et al. 2006).

3.2 *In-flight excavator*

The in-flight excavator developed by Toyosawa et al. (1998) was used in this paper. In this test, for the excavation, this excavator can rake the soil horizontally by using a cutting blade. The movement of the in-flight excavator was controlled manually from the centrifuge operation room which is in the upstairs of the centrifuge. The model ground was excavated in steps up to the occurrence of collapse, where the excavated height of each step was about 5mm or 6 mm.

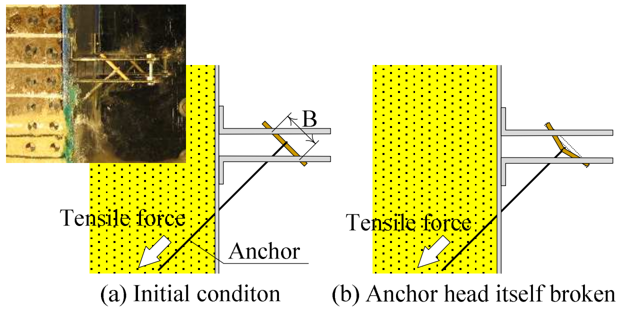

Fig. 8 Physical modelling of broken anchor head

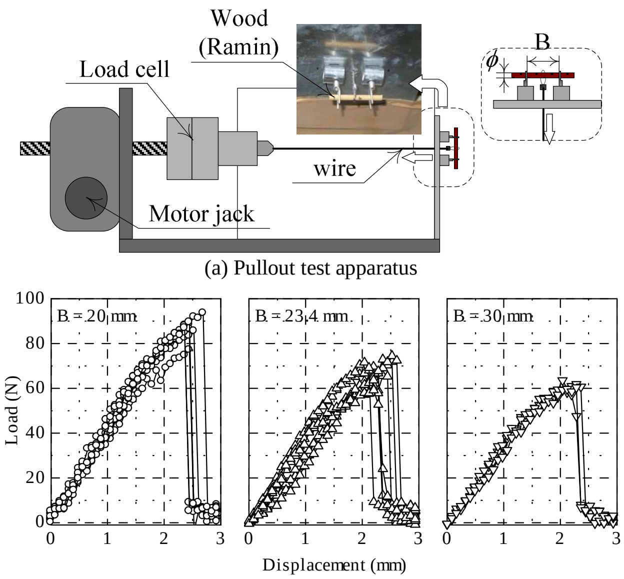

(b) Load – displacement curves in pullout test
Fig. 9 pullout test

3.3 *Model preparation*

From the boring log of the construction site shown in Figure 2, the excavation site consists mainly of Kanto loam (a kind of volcanic cohesive soil in Japan), sand and silt layers. In this paper, (1) a unit layer of sand, and (2) a strata of Kanto loam and sand layer were tested.

3.3.1 Sand layer

Toyoura sand was poured uniformly into an alminium model box in which wall and anchors had been set. The relative density of sand was about 90 %.

3.3.2 Kanto loam and sand layer

Toyoura sand was poured into the aluminium model box to a designated level. Then Kanto loam was placed and compressed on the sand layer. The profile of the model is illustrated in Fig. 6.

An aluminium model box with internal dimensions of 100 mm (w), 450 mm (l) and 272 mm (h) was used. A Perspex window was installed in one side of the box in order to observe the model during the centrifuge test. The model sheet pile was inserted to the predetermined penetration depth.

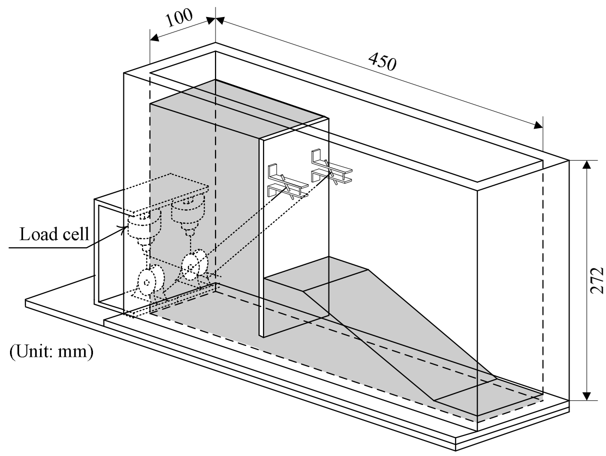

Fig. 10 Model setup

The model anchors, which were 1.0 mm diameter wire ropes through Teflon tubes, were installed at 45 degrees and the ends of wires were connected to the load cells. Figure 7 shows the model of sheet pile (2 mm thick aluminium) with eight earth pressure sensors and six strain gages.

3.4 *Modelling of broken anchor head*

Figure 8 gives the experimental system for the broken anchor head used in this study. The mechanism of the broken anchor head is as follows. It is a problem of a simply supported beam of length B, and cross section, ϕ, carrying a tensile force. A series of pullout tests is carried out to clarify the brittleness of the anchor head model as shown in Fig. 9(a). Fig. 9(b) shows typical examples of how the beam of length B, would change the load - displacement curves for the case of wood (ramin) and cross section, ϕ, of 3mm. Comparing the data obtained from the beam of length B, it can be clearly seen that there is a decreasing maximum load as B increases. In this study, the model anchor head used was wood (ramin), B of 20 mm, ϕ of 3mm from tensile force 90N at failure by Toyosawa (1998).

3.5 *Test procedure*

Figure 10 shows the model setup in the aluminium model box. The sensor's pressure value and bending moment on the model sheet pile were initialized prior to the model setup. Preloading for each anchor was adjusted to 9.8 N before testing. The centrifugal acceleration was then increased to 50g for each test. Once every sensor's value was stable, the excavation started. To simulate the real accident, the ground in front of the model sheet pile was excavated by the in-flight excavator to a depth of 9.5 m near the end of the sheet pile.

4 TEST RESULTS AND DISCUSSIONS

4.1 *Sequence of failure*

Figure 11 shows the profile of each model after failure. Figure 11(a) shows the model with sand layer after failure. During the excavation process, the penetration depth of the wall decreased step by step as excavation proceeded. Failure occurred when the penetration depth of the wall reached about 35 mm and continuous failure with a small displacement emerged with each excavation step. Figure 12 shows the ground displacement field behind the model sheet pile at the final excavation step using PIV (Particle Image Velocimetory, Kikkawa et al. 2006). The failure line angle was about 65 degrees.

The model consisting of Kanto loam and sand layers is shown after collapse in Fig. 11(b). The failure happened suddenly when the penetration depth reached about 60mm. The failure line's angle in the sand was about 65 degree.

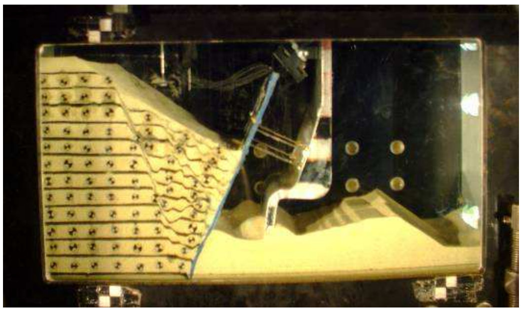

(a) Sand layer

(b) Kanto loam and sand layer
Fig. 11 Profile of models after failure

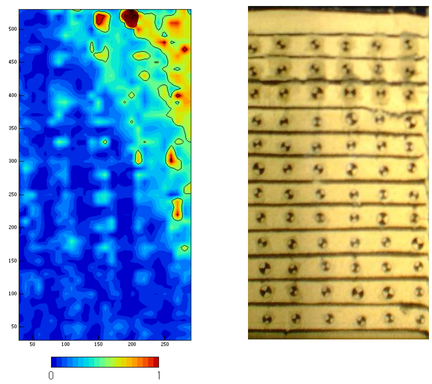

Fig. 12 PIV analysis in the case of the sand layer

4.2 *Earth pressure and bending moment on sheet pile walls*

The measured earth pressure (total lateral stress) on the model sheet pile together with depth during increasing centrifugal acceleration and excavation processes are shown in Fig. 13.

The active and passive earth pressures increased during excavation rather than with increasing centrifugal acceleration. For the sand layer model (Fig. 13(a)), both pressures rapidly increased at an excavation depth of 35mm. For the Kanto loam and sand layer (Fig. 13(b)), the active pressure exceeded 60 kN/m^2 and the passive pressure exceeded 120 kN/m^2 at an excavation depth of 60mm.

The variations of the bending moment with the depth of wall are shown in Fig. 14. The bending moment increased almost uniformly as the centrifugal acceleration increased. On the other hand, during excavation, the moment at the middle of the pile rapidly increased while the moment of the pile at the excavation surface decreased as the excavation depth increased. Therefore, the pile was bent significantly as the upper part of the pile stuck out while the pile at the excavation surface did not move much. This suggested that the anchor head suffered severe tensile force due to the bent pile.

4.3 *Tensile force acting on anchor*

Figure 15 shows the measured tensile force acting on the anchor with increasing centrifugal acceleration and excavation steps. The values in this figure were the average of the two anchors which were set in one model.

The tensile force increased with increasing acceleration in each test. During the excavation process, tensile force increased gradually prior to the failure in both cases. It should be noted that those tensile forces were almost the same as the capacity of the anchor head as shown in Fig. 9, or had already exceeded the capacity.

Therefore, it is believed that the active and passive earth pressures increased during excavation and then caused the anchor head to break. As a result the retaining wall and the ground behind the wall collapsed suddenly.

5 CONCLUSIONS

In this study, the case history of the labour accident involving the collapse of the anchored retaining wall was introduced. In order to understand the mechanism of the accident, we performed the centrifuge model tests in which model ground in front of the anchored retaining wall was excavated using an in-flight excavator.

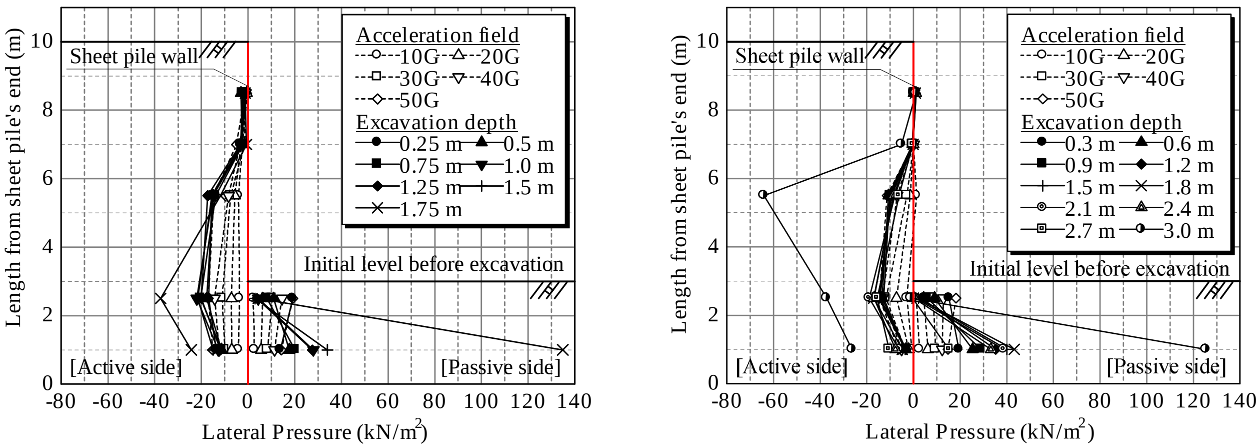

(a) Lateral pressure on wall (Sand layer)

(b) Lateral pressure on wall (Kanto loam and sand layer)

Fig. 13 Lateral pressure on wall

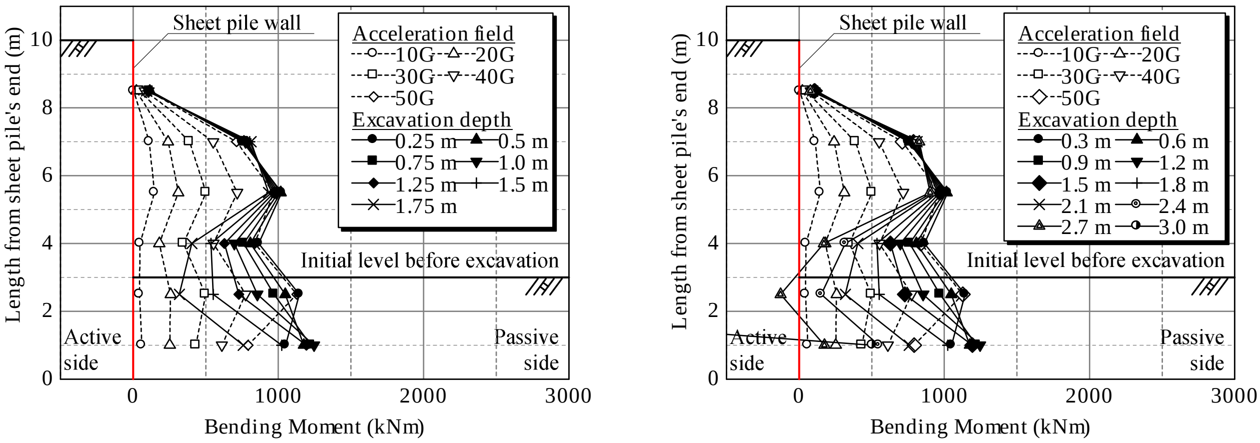

(a) Bending moment at wall (Sand layer)

(b) Bending moment at wall (Kanto loam and sand layer)

Fig. 14 Bending moment at wall

Based on the results of centrifuge model tests, it was revealed that the active and passive earth pressures in the retaining wall increased during excavation and the anchor head exceeded the capacity with respect to the tensile stress. As a result, the retaining wall and ground behind the wall collapsed suddenly.

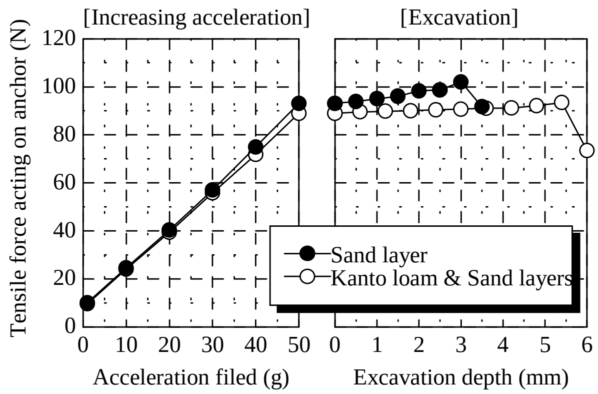

Fig. 15 Tensile force with increasing centrifugal acceleration field and excavation steps

REFERENCES

Toyosawa, Y., Horii, N., Tamate, S., Suemasa, N., and Katada, T. (1998). "Failure mechanism of anchored retaining wall." *Proc., Int. Conf. Centrifuge 98*, Tokyo, Rotterdam, Balkema, pp.667-672.

Toyosawa, Y., Horii, N., Tamate, S. and Suemasa, N. (1996). "Failure characteristics of sheet pile wall in centrifuge tests." *Proc., Geotechnical aspects of underground construction in soft ground*, Balkema, pp.225-230.

Horii, N., Itoh, K., Toyosawa, Y. and Tamate, S. 2006. Development of the NIIS Mark-II geotechnical centrifuge, the 6th International Conference on Physical Modelling in Geotechnics, Ng, Zhang and Wang (eds.), Taylor & Francis, pp. 141-146.

Kikkawa, N., Nakata, Y., Hyodo, M., Murata, H., and Nishio, S. 2006. Three-dimensional measurement of local strain using digital stereo photogrammetry in the triaxil test, Hyodo, Murata and Nakata (eds.), Taylor & Francis, pp. 61-67.